In-structure shock of underground structures : a theoretical approach

Ma, Guowei; Zhou, Hongyuan; Lu, Yong; Chong, Karen

2010

Ma, G.W., Zhou, H.Y., Lu, Y. & Chong, K. (2010). In-structure shock of underground structures : a theoretical approach. Engineering Structures, 32(12), 3836–3844.

https://hdl.handle.net/10356/94968

https://doi.org/10.1016/j.engstruct.2010.08.026

In-structure shock of underground structures: A theoretical approach

Guowei Ma [a,*], Hongyuan Zhou [a], Yong Lu [b], Karen Chong [c]

[a] *School of Civil and Environmental Engineering, Nanyang Technological University, Nanyang Avenue, Singapore 639798, Singapore*

[b] *Institute for Infrastructure and Environment, School of Engineering, The University of Edinburgh, Edinburgh EH9 3JL, UK*

[c] *Defense Science and Technology Agency, Ministry of Defense, 1 Depot Road, Singapore 109679, Singapore*

Abstract: When an underground structure is subjected to a subsurface explosion, an in-structure shock occurs. The in-structure shock can be a major cause of disruption and even damage to the instruments and equipment contained in the structure if the detonation is relatively distant. For this reason, an appropriate analysis and prediction of explosion-induced in-structure shock is an important topic in the area of protective design of underground structures. In this paper, a detailed analysis is conducted on a representative buried structural element subjected to soil-transmitted blast. The soil-structure interactions are considered by introducing an interfacial damping between the structural element and the surrounding soil. Two phases of the structural response to the blast load, i.e., a blast loading phase and a free-vibration phase, are analyzed. Based on the analytically derived time histories of the structural response, which represent the in-structure shock, the response spectra concerning the equipment (sub-structures) attached to the main structure are constructed. Besides providing a theoretical approach for the evaluation of the in-structure shock and its subsequent effects, the present analysis is supplementary to the relevant provisions in *TM5-855-1* and *TM5-1300*, in which only rough predictions of in-structure shock for buried structures are specified.

Keywords: In-structure shock, Buried structure, Soil-structure interaction, Response spectrum, Blast load, Protective design.

Notation

A	Cross-sectional area of the beam
c_s	Acoustic velocity of the surrounding soil
E	Young's modulus
EI	Flexural rigidity of the beam
f	Coupling factor of the explosion energy to soil
l	Length of the beam
m	Attenuation coefficient of blast wave in soil
P_0	Free-field peak pressure
$q_n(t)$	nth mode general coordinate
R	Distance from center of explosion to structure
t	Time
t_a	Travel time of shock wave from detonation to structure
T_d	Blast time duration
t_1	Start time of free vibration of the beam
$w(x,t)$	Displacement of the beam
$w_n(x,t)$	nth mode contribution to displacement of the beam
W	TNT equivalent charge weight
$W_n(x)$	nth mode shape
x	Coordinate along the beam
α	Reduction factor
β	A factor equal to 160 in imperial unit system
$\sigma_f(t)$	Free-field pressure time history

ρ	Mass density of the beam
ρ_s	Mass density of the surrounding soil
ω_n	*n*th mode natural frequency of the beam
ς_n	*n*th mode interfacial damping ratio
v	Poisson's ratio

1. Introduction

When subjected to subsurface explosions, structures buried underground are much safer than those exposed aboveground since the surrounding soil dissipates the shock wave energy significantly. When an underground detonation occurs, a shock wave is generated which propagates in all directions in soil and attenuates rapidly with the increase of the distance from the charge center and may damage surface structures [1, 2]. Provided a certain standoff, the underground structure itself may survive the explosion, but the instruments and equipment contained within the structure may sustain damage due to the effect of the in-structure shock. Indeed, some of the equipment is delicate and vulnerable to such kind of shock load.

In early years, only the rigid body motion of a buried structure was considered in the analysis of the in-structure shock [e.g. 3-6]. With the development of the warhead penetration capacity in the past decades, a subsurface explosion becomes a dominant threat to an underground structure. Consequently, the in-structure shock induced by the local structural response becomes a major concern to the safety of the interior contents (see Fig. 1). When the blast wave encounters an underground structure, it may cause a sudden motion of the local structural element, which in turn acts as an excitation to the equipment attached to the structure. If the specified shock-load tolerance of the equipment is lower than the excitation shock level, the equipment may lose its functions.

In the derivation of the shock level for the equipment, the most important and difficult part is to obtain the response of the structural element under blast load due to the presence of soil-structure interaction (SSI). To determine the underground structure response to subsurface explosions by experimental studies can be very costly. Moreover, it

is almost impossible to carry out parametric studies to identify the critical parameters by experiments. For these reasons, researchers have increasingly resorted to numerical simulations for the detailed investigation of the structural response to shock and blast loads.

Various numerical methods have been employed to simulate underground explosion induced shock wave and its interactions with underground structures. For example, Stamos and Beskos [7] used the boundary element method (BEM) to analyze the dynamic response of large three-dimensional underground structures to external or internal dynamic forces or seismic waves. In their study, the BEM is applied in conjunction with the Laplace transform for soil, structure, as well as dynamic SSI. Yang [8] used the commercial finite element method (FEM) software ABAQUS to investigate the shock response of a monolithic box made of reinforced walls and slabs. The FEM model parameters were established by modifying the existing empirical formulae available for free-field conditions. To improve the efficiency in the numerical modeling, some studies adopted a combined finite difference/finite element method with a sub-structure approach to solve the nonlinear SSI problems [e.g. 9, 10]. More recently, with the development of meshless methods, a combined smoothed particle hydrodynamics (SPH)/FEM model was applied to study the shock response of a box-shaped underground structure subjected to a subsurface blast load [11, 12]. The SPH technique was adopted where large deformation took place, while the traditional FEM was used to model the rest region of the soil and structure.

One significant advantage of the numerical methods is that complex geometrical configurations and material properties can be modeled readily. However, a common difficulty in the numerical simulations is the determination of the model parameters.

Furthermore, analysis using numerical methods is generally very computationally expensive, especially when carrying out parametric studies.

The *Fundamentals of protective design for conventional weapons* (*TM5-855-1*) [3] and the *Structures to resist the effects of accidental explosions* (*TM5-1300*) [4] are two major design codes which may be considered when evaluating the underground structure shock level. However, the method adopted in these codes appears to be overly simplified, in that the structure as a whole is treated as a rigid body for the calculation of the in-structure acceleration, velocity, and displacement by modifying the corresponding free-field values. For example, the acceleration of the structure is obtained by integrating the acceleration-range function over the span of the structure, without considering any structural response and the SSI. To overcome the drawback, some studies proposed the incorporation of the structural response and SSI effects. For example, Wong and Weidlinger [13] considered the structural response to modify the load acting on the structure. Dancygier and Karinski [14, 15] studied an underground cylindrical structure subjected to a surface dynamic load and a buried structure under surface steady-state repetitive load, in which the soil shear resistance and arching effect were incorporated.

For the sake of design applications, most of the analytical approaches for the dynamic response of underground buried structures have been based on single-degree-of-freedom (SDOF) models. The corresponding SDOF modeling approaches may be grouped in two categories: a) rigid body SDOF, where the entire structure embedded in soil is treated as a rigid body and responded to a blast load in one direction only [e.g. 5, 6]; b) equivalent SDOF mass-spring system, usually representing the response (deflection) of structural members such as a floor or wall subjected to a blast load [e.g. 16]. Clearly, the

adequacy of using a SDOF model to represent an underground structure or structural component will largely depend on an appropriate equivalent treatment of the SSI. However, this is not always possible because the effect of SSI is closely associated with the response profile at the soil-structure interface in a point-wise manner, which is difficult to be represented in a SDOF setting. In this regard, a continuous model becomes necessary.

The present study is aimed to develop an integrated analytical model for the prediction of the in-structure shock of buried structures, taking into consideration the shock wave in soil, soil-structure interaction and the structural response. The essential response of the structure is represented by a beam model, while the SSI is incorporated by means of interfacial damping. For simplification and without losing generality, it is assumed that the detonation is at a certain distance away from the buried structure and so there is no significant structural damage to the buried structure. Furthermore, the burial depth is assumed to be sufficient so that there is no wave reflection from the ground surface. With the solution of the structural response, the response spectra for the sub-structures attached to the main structure are constructed. Such in-structure shock response spectra may be used to supplement *TM5-855-1* and *TM5-1300* [3, 4] for a more realistic in-structure shock analysis and design.

2. Underground explosion induced shock load and soil-structure interaction

The intensity of the free-field stress wave generated by an underground detonation of conventional weapons may be estimated by a semi-empirical formula given in *TM5-855-1* [3] as follows,

$$P_0 = \beta f\left(\rho_s c_s\right)\left(\frac{R}{W^{1/3}}\right)^{-m} \tag{1}$$

where P_0 is the free-field peak pressure, in psi; f is a coupling factor of the explosion energy to soil, dimensionless; $\rho_s c_s$ is the acoustic impedance of soil, in psi/fps; m is an attenuation coefficient, dimensionless; W is the TNT equivalent charge weight, in lb; R is the distance measured from the center of explosion to the structure, in ft; and β is a factor equal to 160 in the imperial unit system, dimensionless. It should be noted that the pressure calculated in psi is converted to SI unit system in Pa before being used in the following.

The shape of the shock wave propagating in soil resembles that of the charge. If the detonation is far from the structure as compared to the characteristic dimension of the structure, the curvature of the shock wave surface may be ignored, so that the load applied on the structure can be approximated as a plane wave, in which the arrival time difference of the actual wave to the structure is also neglected thus the pulse is a function of only time. In engineering practice, an equivalent uniform pressure is applied by multiplying the peak value with a reduction factor based on the actual load distribution. For a rectangular structural member, the factor can be readily obtained [3].

The temporal variation of the pressure generated by an underground explosion may be approximated by an exponential decaying law [5], i.e.

$$P\left(t\right) = P_0 \alpha e^{-t/t_a} \tag{2}$$

where t_a is the travel time of the shock wave from the detonation point to the structure; α is a reduction factor, defined as ratio of the equivalent uniform pressure on a wall or floor of the structure to the maximum pressure of the actual load distribution. When the detonation

is relatively distant, the pressure distribution is very close to that of a plane wave and the reduction factor is nearly 1. In engineering practice, the pressure time history is usually further simplified as a triangular load, such that

$$\sigma_f(t) = \begin{cases} P_0\alpha\left(1-\dfrac{t}{T_d}\right) & for\ t \le T_d \\ 0 & for\ t > T_d \end{cases} \tag{3a}$$

where T_d is the equivalent blast time duration in the triangular simplification. Preserving the impulse and peak pressure as in the exponentially decreasing load yields

$$T_d = \frac{\int_0^\infty P_0\alpha e^{-t/t_a}dt}{\frac{1}{2}P_0\alpha} = 2t_a \tag{3b}$$

When the blast stress wave intersects a solid structure, the peak pressure exerted on the front face of the structure or structural element is amplified due to the refection effect. *TM5-855-1* [3] recommends that the peak pressure of the stress wave acting on the structural element be 1.5 times that of the respective free-field value [3]. However, this recommendation does not consider the difference in soil types and structural stiffness, and hence is a rather crude estimation.

A more rigorous treatment may be achieved by considering the acoustic theory in the analysis [17]. As a stress wave propagates and reaches an interface of two different materials, it will be partially transmitted and partially reflected. At the interface, the equilibrium condition and the continuous condition must be satisfied. Consequently, when the shock wave arrives at an interface with a structure, the pressure applied on the structure is the sum of the free-field pressure (σ_f) plus the reflected pressure (σ_c) [5, 13], as

$$\sigma = \sigma_f + \sigma_c = 2\sigma_f - \rho_s c_s \dot{u} \tag{4}$$

where $\dot{u}$ is the particle velocity of a structure material point. It is worth noting that the above formula is valid only in the time period when the particle velocity in the soil is higher than that in the structure around the interface. This normally happens within the blast wave duration. When the particle velocity of soil is less than that of the structural element at the interface, the interaction between soil and structure vanishes and the pressure exerted on the structural element becomes zero.

Eq. (4) is employed to represent the soil-structure interaction in the present model for the in-structure shock, as will be described later.

3. Euler beam model

Buried structures are typically in a box-shape. Generally speaking, the response of an element of a box structure may be better represented by a plate or a slab model. As far as the governing in-structure shock is concerned, however, if the dimension of one edge is larger than twice that of the other, it is possible and convenient to further simplify the slab into a beam model, as shown in Fig. 1. This is reasonable because the most severe in-structure shock is expected to take place in the middle section of the structure. Thus, by taking a strip of unit width parallel to the shorter edges of a wall or floor, a beam model can be established to represent the out-of-plane response of the rectangular structural member.

To simplify the solution, Euler beam theory is adopted here. The governing equation for a beam under the soil-transmitted blast pressure loading can be written as

$$EI\frac{\partial^4 w(x,t)}{\partial x^4}+\rho A\frac{\partial^2 w(x,t)}{\partial t^2}+\rho_s c_s\frac{\partial w(x,t)}{\partial t}=2P_0\alpha\left(1-\frac{t}{T_d}\right) \tag{5}$$

where $w(x,t)$ is the displacement of the beam, which is a function of the location x and time t; EI, ρ, and A are the flexural rigidity, density, and area of the cross-section of the beam, respectively; Thus, the soil-structure interaction is incorporated into the formulation of the structural response (in-structure shock). For the elastic response of the beam, the solution of the displacement can be obtained by modal superposition, as

$$w(x,t)=\sum_{n=1}^{\infty}W_n(x)q_n(t) \tag{6}$$

where $W_n(x)$ is the nth mode shape, and $q_n(t)$ is the nth generalized modal coordinate. From the governing equation, and assuming a simply supported boundary condition (other support conditions may be considered in a similar way if necessary), the nth mode can be determined as

$$W_n(x)=\sqrt{\frac{2}{\rho Al}}\sin\frac{n\pi x}{l} \tag{7}$$

where l is the length of the beam; n is an integer from 1 to infinity denoting the orders of the modes.

In fact, for the six slabs of a RC box structure, the connection of any one to its adjacent four slabs is neither fixed nor simply supported: it is less rigid than fixed boundary and more rigid than simply supported boundary. However, simply supported boundary, employed in this paper, gives conservative predictions so that in engineering practice, safer.

4. Shock load response analysis

The response of a structural member to a transient blast load consists of two phases, namely, a loading phase and a free vibration phase.

4.1 Shock response within the blast duration

For the response within the blast duration, substituting Eq. (6) into Eq. (5) and rewriting leads to

$$\rho A\sum_{n=1}^{\infty}\omega_n{}^2 W_n(x)q_n(t)+\rho A\sum_{n=1}^{\infty}W_n(x)\ddot{q}_n(t)+\rho_s c_s\sum_{n=1}^{\infty}W_n(x)\dot{q}_n(t)=2P_0\alpha\left(1-\frac{t}{T_d}\right) \tag{8}$$

where $\omega_n=\sqrt{\frac{EI}{\rho A}}\left(\frac{n\pi}{l}\right)^2$ is the *n*th natural frequency of the beam. Using the orthogonal property of modes, the equation of motion for the *n*th mode in the generalized coordinate space can be expressed as

$$\ddot{q}_n(t)+\frac{\rho_s c_s}{\rho A}\dot{q}_n(t)+\omega_n^2 q_n(t)=2\left[1-(-1)^n\right]\frac{l}{n\pi}\sqrt{\frac{2}{\rho Al}}P_0\alpha\left(1-\frac{t}{T_d}\right) \tag{9}$$

It can be seen that the interaction effect from the soil and the structure manifests as a damping. An interfacial damping ratio of the system can then be defined as

$$\zeta_n=\frac{\frac{\rho_s c_s}{\rho A}}{2\omega_n}=\frac{\frac{\rho_s c_s}{\rho A}}{2\sqrt{\frac{EI}{\rho A}}\left(\frac{n\pi}{l}\right)^2} \tag{10}$$

Substituting Eq. (10) into Eq. (9), the governing equation for the general mode can be written as

$$\ddot{q}_n(t)+2\zeta_n\omega_n\dot{q}_n(t)+\omega_n^2 q_n(t)=2\left[1-(-1)^n\right]\frac{l}{n\pi}\sqrt{\frac{2}{\rho Al}}P_0\alpha\left(1-\frac{t}{T_d}\right) \tag{11}$$

The interfacial damping effectively represents the soil-structure interaction and it depends on the properties of both the structure and surrounding soil. Among the influencing factors are the acoustic impedance of soil as well as the structural element properties such as density, area of the cross-section, flexural rigidity and length. It should be noted that the interfacial damping ratio of the system decreases with the order of modes which means the interfacial damping effect have greater influence on lower modes and less influence on higher modes. For reinforced concrete structure buried in typical soils with density ranging from 1000 kg/m^3 to 2000 kg/m^3 and seismic velocity ranging from 300 m/s to 2000 m/s, the interfacial damping ratios of the first or first several modes are usually larger than 1, while those for the higher modes are less than 1. The continuous beam model has obvious advantage over the SDOF model in the consideration of the SSI. The effect of the interfacial damping on different vibration modes can also be reflected by the continuous beam model. The general coordinate for all modes with different interfacial damping ratio will be derived in the following.

4.2 Case I: $\xi_n \geq 1$

Let the arrival time of the blast load be time zero. Hence, at time zero both the initial displacement and velocity of the beam are zero,

$$w(x,0) = 0,\ \dot{w}(x,0) = 0 \tag{12}$$

The initial conditions in the generalized coordinate space can be written as

$$q_n(0) = \int_0^l \rho A W_n(x)\, w(x,0)\, dx = 0,\ \dot{q}_n(0) = \int_0^l \rho A W_n(x)\, \dot{w}(x,0)\, dx = 0 \tag{13}$$

Solve Eq. (11) with the initial conditions and recall Eq. (6) and Eq. (7), for an interfacial damping ratio larger than or equal to 1, the contribution of the *n*th mode to the displacement of the structural element is

$$w_n(x,t)=\sqrt{\frac{2}{\rho Al}}\sin\frac{n\pi x}{l}\left[E_n e^{D_{n,2}t}+F_n e^{D_{n,3}t}+2D_{n,1}\left(1-\frac{t}{T_d}+\frac{2\zeta_n}{\omega_n T_d}\right)\right] \tag{14}$$

where

$$E_n=\frac{D_{n,1}\left[1+\left(T_d+\frac{2\zeta_n}{\omega_n}\right)D_{n,3}\right]}{\omega_n T_d\sqrt{\zeta_n^2-1}},\ F_n=-\frac{D_{n,1}\left[1+\left(T_d+\frac{2\zeta_n}{\omega_n}\right)D_{n,2}\right]}{\omega_n T_d\sqrt{\zeta_n^2-1}}$$

$$D_{n,1}=\left[1-(-1)^n\right]\frac{l}{n\pi}\sqrt{\frac{2}{\rho Al}}\frac{P_0\alpha}{\omega_n^2},\ D_{n,2}=\left(-\zeta_n+\sqrt{\zeta_n^2-1}\right)\omega_n,\ D_{n,3}=\left(-\zeta_n-\sqrt{\zeta_n^2-1}\right)\omega_n$$

Subsequently,

$$\dot{w}_n(x,t)=\sqrt{\frac{2}{\rho Al}}\sin\frac{n\pi x}{l}\left(E_n D_{n,2}e^{D_{n,2}t}+F_n D_{n,3}e^{D_{n,3}t}-\frac{2D_{n,1}}{T_d}\right) \tag{15}$$

$$\ddot{w}_n(x,t)=\sqrt{\frac{2}{\rho Al}}\sin\frac{n\pi x}{l}\left(E_n D_{n,2}^2e^{D_{n,2}t}+F_n D_{n,3}^2e^{D_{n,3}t}\right) \tag{16}$$

It should be mentioned that the above solutions (displacement, velocity and acceleration contributions) are valid only within the time overlap of the blast duration and the time period ranging from zero to the maximum displacement.

4.3 Case II: $\zeta_n<1$

When the interfacial damping ratio is smaller than 1, the *n*th order motion contribution to the displacement variable can be written as

$$w_n(x,t)=\sqrt{\frac{2}{\rho Al}}\sin\frac{n\pi x}{l}\left\{e^{-\zeta_n\omega_n t}\left[E_n\sin\left(D_{n,4}t\right)+F_n\cos\left(D_{n,4}t\right)\right]+2D_{n,1}\left(1-\frac{t}{T_d}+\frac{2\zeta_n}{\omega_n T_d}\right)\right\} \tag{17}$$

where

$$E_n=\frac{2D_{n,1}}{D_{n,4}T_d}\left[1-\zeta_n\omega_n\left(T_d+\frac{2\zeta_n}{\omega_n}\right)\right],\ F_n=-2D_{n,1}\left(1+\frac{2\zeta_n}{\omega_n T_d}\right),\ D_{n,4}=\sqrt{1-\zeta_n^2}\,\omega_n$$

Subsequently,

$$\dot{w}_n(x,t)=\sqrt{\frac{2}{\rho Al}}\sin\left(\frac{n\pi x}{l}\right)\left\{e^{-\zeta_n\omega_n t}\begin{bmatrix}-\left(\zeta_n\omega_n E_n+D_{n,4}F_n\right)\sin\left(D_{n,4}t\right)\\+\left(D_{n,4}E_n-\zeta_n\omega_n F_n\right)\cos\left(D_{n,4}t\right)\end{bmatrix}-\frac{2D_{n,1}}{T_d}\right\} \tag{18}$$

$$\ddot{w}(x,t)=\sqrt{\frac{2}{\rho Al}}\sin\frac{n\pi x}{l}e^{-\zeta_n\omega_n t}\begin{Bmatrix}\left[\omega_n^2E_n\left(2\zeta_n^2-1\right)+2\omega_n\zeta_nF_nD_{n,4}\right]\sin\left(D_{n,4}t\right)+\\\left[-2\omega_n\zeta_nD_{n,4}E_n+\omega_n^2F_n\left(2\zeta_n^2-1\right)\right]\cos\left(D_{n,4}t\right)\end{Bmatrix} \tag{19}$$

Again the solutions are valid only within the time intersection of the blast duration and time period ranging from zero to maximum displacement.

The total displacement, velocity, and acceleration of the structural element should be the summation of contributions from different modes, i.e.,

$$w(x,t)=\sum_{n=1}^{\infty}W_n(x)q_n(t),$$

$$\dot{w}(x,t)=\sum_{n=1}^{\infty}W_n(x)\dot{q}_n(t),$$

$$\ddot{w}(x,t)=\sum_{n=1}^{\infty}W_n(x)\ddot{q}_n(t) \tag{20}$$

4.4 Free vibration

After the shock load duration is completed, the SSI vanishes and the interfacial damping ratio becomes zero. The governing equation for the generalized coordinate during the free vibration is

$$\ddot{q}_n\left(t_1\right)+\omega_n^2 q_n\left(t_1\right)=0 \tag{21}$$

Offsetting the time by the blast duration and defining $t_1=t-T_d$ for the free vibration phase, the initial condition for t_1 is actually the terminal condition of the shock load duration. Thus, the displacement, velocity and acceleration responses of the structural element after the shock load phase are, respectively:

$$w\left(x,t_1\right)=\sum_{n=1}^{\infty}\sqrt{\frac{2}{\rho Al}}\sin\frac{n\pi x}{l}\left[\frac{\dot{q}_n\left(t_1=0\right)}{\omega_n}\sin\omega_n t_1+q_n\left(t_1=0\right)\cos\omega_n t_1\right] \tag{22}$$

$$\dot{w}\left(x,t_1\right)=\sum_{n=1}^{\infty}\sqrt{\frac{2}{\rho Al}}\sin\frac{n\pi x}{l}\left[\dot{q}_n\left(t_1=0\right)\cos\omega_n t_1-\omega_n q_n\left(t_1=0\right)\sin\omega_n t_1\right] \tag{23}$$

$$\ddot{w}\left(x,t_1\right)=\sum_{n=1}^{\infty}\sqrt{\frac{2}{\rho Al}}\sin\frac{n\pi x}{l}\left[-\omega_n\dot{q}_n\left(t_1=0\right)\sin\omega_n t_1-\omega_n^2 q_n\left(t_1=0\right)\cos\omega_n t_1\right] \tag{24}$$

It should be highlighted that t_1 is the start time of free vibration and the solution is applicable from that time until the displacement reaches its maximum value (if the displacement does not reach its peak value in the blast duration). In an underground shock scenario, the maximum velocity and acceleration of the structural element are generally achieved within this period and then the responses will attenuate quickly with time. In fact, the chance of the structural member rebounding and interacting again with the surrounding soil do exists. If this happens, the equations in section 4 will fail. Therefore the equations

are valid before the rebound happens, in other words, they are valid until the displacement reaches its maximum value.

Further, under a subsurface detonation, both the rigid body motion of the entire structure and the local deflection of structural member occur. It is very interesting to discuss in-structure shock of underground structures subjected to subsurface detonation with both effects from local deflection and overall response-rigid body motion. However, in some situations, e.g. the hollow box structure is relatively large and heavy, the local deflection dominates and rigid body motion effect is insignificant, just as discussed in the present study. In the future study, more generally, the rigid body motion of the entire structure will be incorporated into the model and its contribution in the in-structure shock will be analyzed.

5. Example shock response analysis using continuous beam model

Consider a box-shaped underground buried structure subjected to a shock load on one side of the structure. It is assumed that the structure is buried in a significant depth so that the reflections from soil surface can be ignored. The whole structure is made of reinforced concrete (RC), and the dimensions of the wall or floor under consideration are 12.8 m×26 m×1 m. Considering the convention of one-way slab, the span of the beam model is 12.8 m and the cross-sectional area is 1 m^2 (1 m by 1 m). The RC has a Young's modulus of 30 GPa and Poisson's ratio of 0.2 as well as density of 2500 kg/m^3. To represent the one-way slab, the beam model is in a plane strain manner, in which the Young's modulus is

modified as $E/(1-\nu^2)$, with a value of 31.25 GPa. Three typical soils in Singapore are used, namely dry sand, Kallang soil and Bukit Timah soil (Kallang soil is a kind of clay while Bukit Timah soil is a kind of residual soil [18]), whose properties are listed in Table 1. The explosion scenario considered is a scaled distance (stand-off distance divided by the cube root of the TNT equivalent charge weight) of 2 $m/kg^{1/3}$. It is assumed that the detonation is relatively distant from the structure, a reduction factor of 0.8 is used; the equivalent plane wave peak pressures in three soils are calculated from Eq. (1) and the reduction factor. The blast load on the buried structure is evaluated to have duration of approximately 20 ms, typical for subsurface blasts [18].

According to the formulation in Section 4, the interfacial damping ratio is evaluated as follows. With the Kallang soil, the beam model is over-damped with the first three vibration modes and the interfacial damping ratios are 9.86, 2.47 and 1.10, respectively; for higher modes, the system is under-damped, with a decreasing interfacial damping ratio as 0.62, 0.39, and so on. However, in the case of dry sand, which has smaller acoustic impedance, only the first mode of the system is interfacially over-damped while other modes are interfacially under-damped. The detailed interfacial damping ratios with respect to the three typical soils are summarized in Table 2.

The time histories of displacements, velocities and accelerations of different points on the structural element can then be obtained following the solutions presented in Section 4. For a conservative consideration, the mid-span response of the beam is particularly studied. As mentioned earlier, the formulae in the present study are valid when the displacement varies from zero to its maximum value, but this is considered to be sufficient

for the evaluation of the critical shock environment within the structure as the response will attenuate rapidly after this time.

Fig. 2 shows the time histories of displacement, velocity and acceleration at the mad-span of the element under three different soil conditions, respectively. It can be observed that under such loading, structural and material conditions, the displacements achieve their maximum values in a very short time after the blast ends, whereas the velocities reach their peak values within the shock load duration. The accelerations attain their peak values instantaneously upon loading and attenuate very quickly. It is worth noting that the maximum accelerations are the most important quantities in the response since they are often used to give a criterion of the in-structure shock.

Different soils have different acoustic impedance, thus resulting in different structural responses. In general, the maximum displacement, velocity and acceleration are higher in soil with larger acoustic impedance than those in soil with smaller impedance. For larger soil acoustic impedance, the structural element achieves its maximum velocity sooner and its acceleration attenuates more quickly. It is of particular importance to note that, comparing to the maximum displacement and the maximum velocity, the maximum acceleration appears to be most sensitive to the soil condition. In a soil with large acoustic impedance, the maximum acceleration can be very high, and this poses the most serious threat to the equipment in the structure. Therefore, it is more desirable that an underground protective structure be constructed at a site where the soil has smaller acoustic impedance. Alternatively, it may be considered to use backfill low impedance soil to surround the buried structure for the purpose of in-structure shock mitigation.

Consider a situation in which all the conditions are the same except that the blast duration is changed to 40 ms. For comparison purpose, only Kallang soil is used. From Fig. 3, the mid-span displacement and velocity under 40 ms blast duration are remarkably higher than those under 20 ms blast duration, respectively. However, it is interesting to observe that the mid-span acceleration time histories under two blast durations are almost same.

Fig. 4 plots the relationship between the maximum responses and the scaled distance. Such plots are very useful in practical applications. All the maximum responses decrease with the scaled distance, as can be expected. However, different from the maximum displacement and velocity, the maximum acceleration decreases with the scaled distance extremely quickly in soil with larger acoustic impedance.

In fact, the load exerts on the structural element only when the soil particle velocity is higher than that of the structure material points. According to the assumption, the characteristic of soil particle velocity induced by the subsurface detonation is that it achieves peak value initially then attenuates to zero in the end of the blast. For the velocity of structure, various positions have different velocity time histories; although magnitudes in different material points differ, the patterns are similar: the velocity achieves peak value quickly from initial condition at rest, then attenuates to nearly zero in the end of the pulse (in case study of a typical underground blast), as shown in Fig. 2. In the whole process, some central points of the structure may experience velocity larger than soil particle velocity in some instants. Therefore for these points the actual load applied on the structural element may have a few peaks due to contact and separation of the structure with the surrounding soil. However, it is assumed that throughout the shock duration, the particle

velocity is larger than that of the structure (in fact, in some instants, this assumption in some points around the mid-span may not be valid), indicating there is no separation between soil and structure, which will results in a conservative prediction.

6. In-structure shock and response spectrum analysis

An in-structure shock model of the underground structure aims to give a comprehensive evaluation of the shock environment within the structure. When the detonation parameters are given, the shock level the equipment will experience can be predicted using such a model.

With the beam model presented in Section 4 and as shown in Section 5, the dynamic response of a buried structure can be calculated in detail in terms of the displacement, velocity and acceleration time histories at any location on the structural element. Subsequently, the shock environment within the structure can be evaluated based on these time histories.

For an equipment unit that is attached to the structure element, the shock excitation essentially comes from the above mentioned dynamic response of the structure. Assuming the mass of the equipment is small as compared to the structural element, the influence of equipment on the structural element can be ignored. Thus the analysis of the equipment response can be uncoupled from the structural response analysis. A device mounted in the structural member is modeled as an SDOF system consisting of mass, spring and damping.

The possible effect of the in-structure shock on the equipment attached to the structure can be well represented by the shock response spectrum, which is a plot of the maximum response of SDOF oscillators subjected to the given input motions against

natural frequencies of the SDOF systems, as schematically illustrated in Fig. 5, indicating that response spectra are constructed from SDOF systems of different frequencies subjected to the same base excitation- in fact the structural member response under subsurface blast. For the equipment response under a pulse excitation with a very short duration, the effect of damping on the maximum response is relatively insignificant and hence may be neglected [19].

Fig. 6 shows the computed in-structure shock response spectra under the explosion scenario described in Section 5, for the case where the structure is surrounded by Kallang soil. As is customary in plotting such response spectra, the tripartite plot is employed, from which the maximum displacement, velocity and acceleration can be obtained readily when the natural frequency of the SDOF system representing the equipment is known. By comparing the spectral response values with the respective tolerance limits for a particular piece of equipment, the safety or possible damage to the equipment can be evaluated.

As the structural response (the beam model) is affected by the soil type, scaled distance of the explosion, and the time duration of the blast load, the shock response spectra are expected to exhibit the influence of these factors as well. Fig. 7 shows three pairs of the shock response spectra for a comparison. It can be observed that equipment will experience greater response when the buried structure is surrounded by soil with larger acoustic impedance (Fig. 7(a)). The equipment also experiences greater response under a closer detonation, as expected. Finally, under shock loads with the same peak pressure but different durations, the equipment responds almost the same since the acceleration time histories of the structural element of different blast durations, attenuating quickly within a

very short duration, are almost the same due to the presence of the interfacial damping, shown in Fig. 3 and Fig. 7.

Consider the dimensions of the example box structure to be 12.8 m×26 m×8 m with a wall or floor thickness of 1 m, buried in Kallang soil. The structural member of 12.8 m by 26 m is subjected to a pulse with a scaled distance of 2 m/kg$^{1/3}$. According to *TM5-855-1* [3], the maximum acceleration of the whole structure would be 27 g and the maximum acceleration of the equipment would be 54 g. However, from the present analysis as described in the previous section, the maximum acceleration of the structural element is found to be 82 g at the mid-span, as shown in Fig. 2. Moreover, based on the shock spectrum analysis results, the spectral acceleration of an equipment piece will range from 0.01g to about 70 g, depending on its natural frequency. Clearly, because of the ignorance of the structural dynamic response, *TM5-855-1* is incapable of providing a comprehensive prediction of in-structure shock and the equipment responses, and in some situations, the prediction by *TM5-855-1* may underestimate the actual responses.

Table 3 lists some typical limit values of equipment shock resistance [3]. For an illustration, the vertical tolerance of air handling units, diesel engine generators and computers are plotted in Fig. 6 and Fig. 7. For example, from Fig. 7(a) one can observe that under the blast in the present case, a diesel engine generator is absolutely safe, regardless of its support condition, if the underground protective structure is buried in dry sand. It can also be inferred from the figures that for the safety of the equipment, the stiffness of the equipment support should be kept less than certain critical values, which can be deduced from the respective natural frequencies identified from these figures.

It should be pointed out that the results discussed in this and the previous sections are applicable to structures having similar characteristics as those considered in this example case study. Nevertheless, the analysis procedure can be extended to structures with different properties, and the trends with regard to the various influence factors are expected to hold under typical buried explosion scenarios.

7. Conclusions

In-structure shock of underground structures subject to subsurface detonation is investigated theoretically using a beam model. The soil-structure interaction is taken into consideration in the dynamic equation by introducing interfacial damping to the system consisting of the structural element and the surrounding soil. The solution of dynamic response of the beam is obtained by means of modal superposition. Based on the time histories of the structural response, the shock response spectra are subsequently constructed, and these shock response spectra provide an effective means for the assessment of the working condition of the equipment mounted on the structural member.

Representative analysis results indicate that the maximum displacement, velocity and acceleration responses are higher when the structure are surrounded by soil with larger acoustic impedance, and this subsequently results in greater equipment shock level. In particular, the maximum acceleration of the structural element increases with the soil acoustic impedance dramatically. Therefore, for acceleration sensitive equipment, the protective structures should be constructed in a site with small impedance and the equipment should be placed near corners within the structure. Most significantly, the present study establishes a method to predict in-structure shock of underground structures

in a detailed and effective way. Factors missing in the crude prediction in *TM5-855-1* such as properties of surrounding soil, the particulars of the underground structure, soil-structure interaction and structural response are considered. Further, the information of equipment and the excitation time history are also incorporated to give accurate predictions for specific devices with different natural frequencies. Although a little bit conservative, the current method can be used as supplement to *TM5-855-1* to give a better prediction of in-structure shock of underground structures. This theoretical model needs experimental verification and validation.

References

[1] Hao H, Ma GW, Lu Y. Damage assessment of masonry infilled RC frames subjected to blasting induced ground excitations. Eng Struct 2002;24: 799-809.

[2] Ma GW, Hao H, Zhou YX. Assessment of structure damage to blasting induced ground motions. Eng Struct 2000;22: 1378-89.

[3] US Army Engineers Waterways Experimental Station. Fundamentals of protective design for conventional weapons, TM5-855-1, Vicksburg, 1986.

[4] Departments of the army, the navy and the air force. Structures to resist the effects of accidental explosions, TM5-1300, 1990.

[5] Weidlinger P, Hinman E. Analysis of underground protective structures. J Struct Eng-ASCE 1988;114 (7): 1658-73.

[6] Alwis WAM, Lam KY. Response spectrum of underground protective structures. Finite Elements Analysis Design 1994;18: 203-09.

[7] Stamos AA, Beskos DE. Dynamic analysis of large 3-D underground structure by the BEM. Earthquake Eng Struct Dynamics 1992;24: 917-34.

[8] Yang W. Finite element simulation of response of buried shelters to blast loadings. Finite Elements Analysis Design 1997;24: 113-32.

[9] Chen Y, Krauthammer T. A combined Adina-finite difference approach with substructure for solving seismically induced nonlinear soil-structure interaction problems. Computers Struct 1989;32 (3-4): 779-85.

[10] Stevens DJ, Krauthammer T. A finite difference/finite element approach to dynamic soil-structure interaction modeling. Computers Struct 1988;29 (2): 199-205.

[11] Wang ZQ, Lu Y, Hao H, Chong K. A full coupled numerical analysis approach for buried structures subjected to subsurface blast. Computers Struct 2005;83: 339-56.

[12] Lu Y, Wang ZQ, Chong K. A comparative study of buried structure in soil subjected to blast load using 2D and 3D numerical simulation. Soil Dynamics Earthquake Eng 2005;25: 275-88.

[13] Wong FS, Weidlinger P. Design of underground protective structures. J Struct Eng-ASCE, 1983;109 (8): 1972-79.

[14] Dancygier AN, Karinski YS. A simple model to assess the effect of soil shear resistance on the response of soil buried structures under dynamic loads. Eng Struct 1999;21: 1055-65.

[15] Dancygier AN, Karinski YS. Response of a buried structure to surface repetitive loading. Eng Struct 1999;21: 416-24.

[16] Chen HL, Chen SE. Dynamic response of shallow-buried flexible plates subjected to impact loading. J Struct Eng-ASCE 1996;122 (1): 55-60.

[17] Smith PD, Hetherington JG. Blast and ballistic loading of structures, Butterworth-Heinemann, London, 1994.

[18] Anand S. Measurement and modeling of ground response due to dynamic loading, PhD thesis, Nanyang Technological University, Singapore, 2007.

[19] Clough RW, Penzien J. Dynamics of structures, McGraw-Hill, New York, 1993.

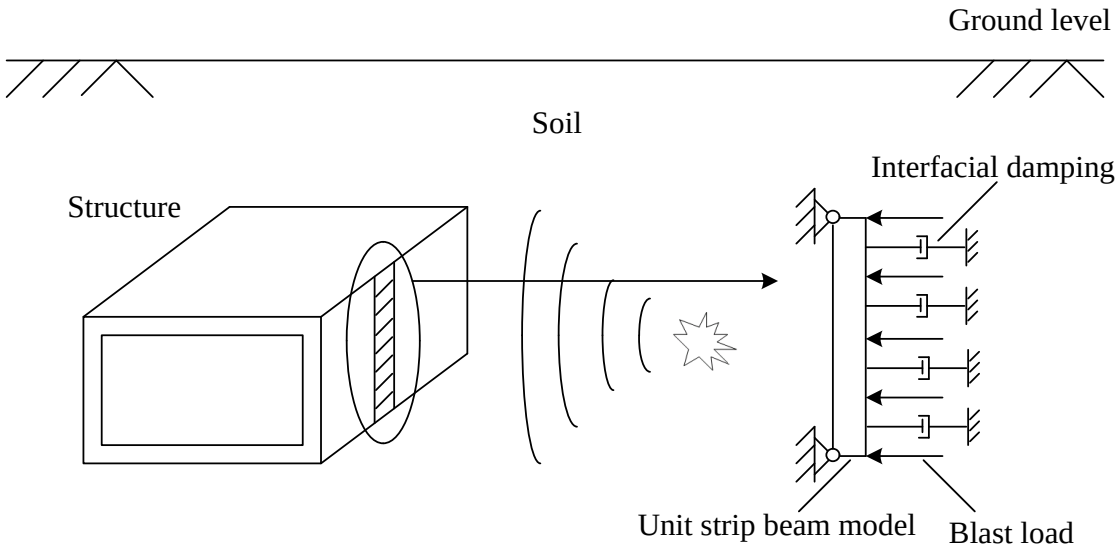

Fig. 1 Underground structure subjected to blast load and simplified analysis model

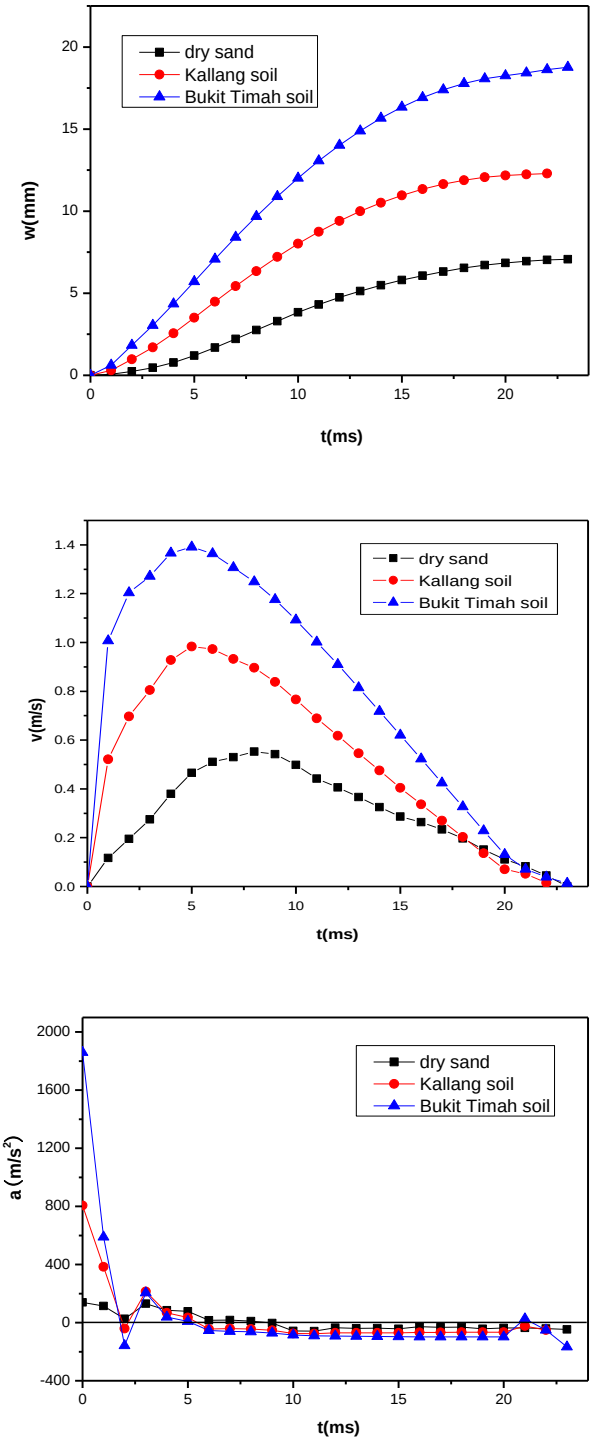

Fig. 2 Time histories of displacement, velocity and acceleration at mid-span of the structural member

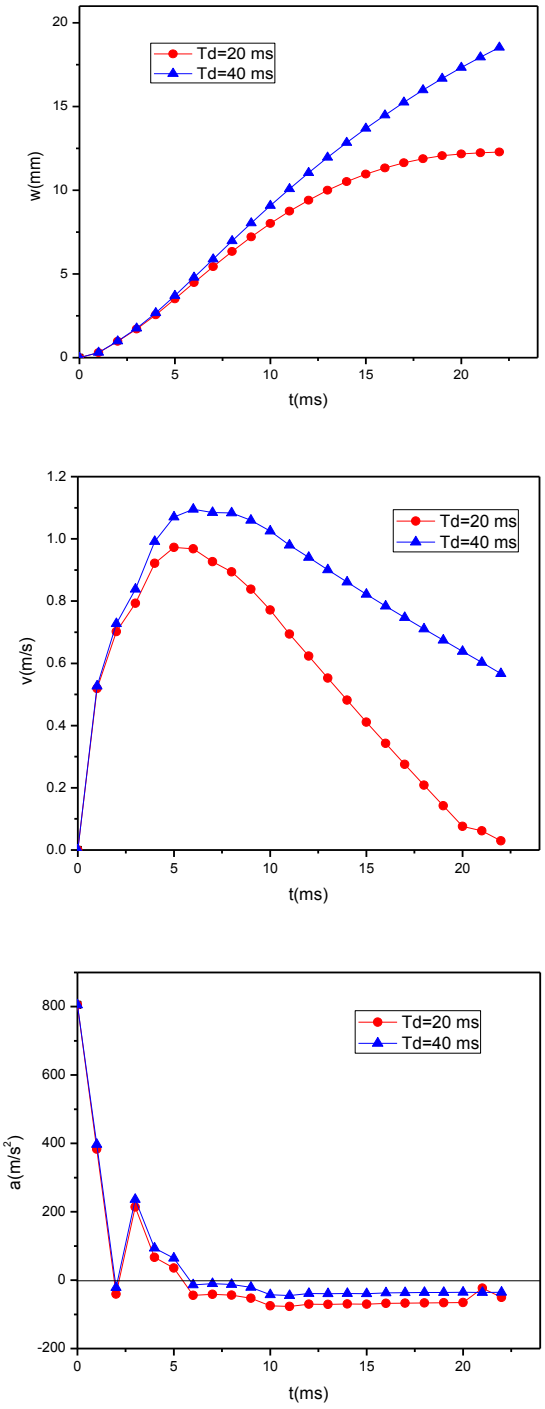

Fig. 3 Mid-span response comparison under different blast durations, Kallang soil

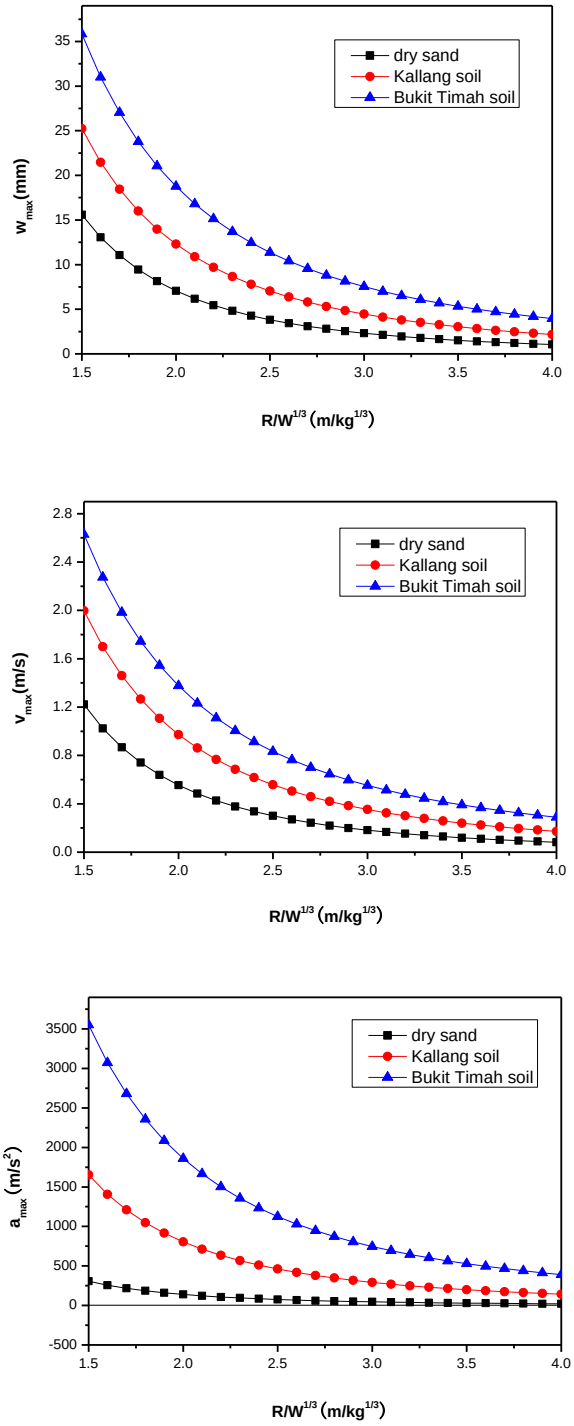

Fig. 4 Maximum displacement, velocity and acceleration at mid-span of the structural member

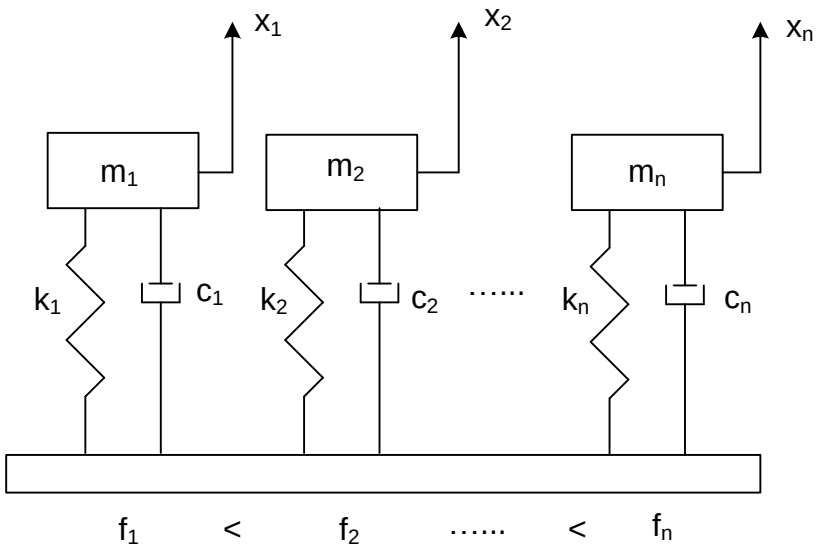

Fig. 5 Schematic illustration of shock response spectra

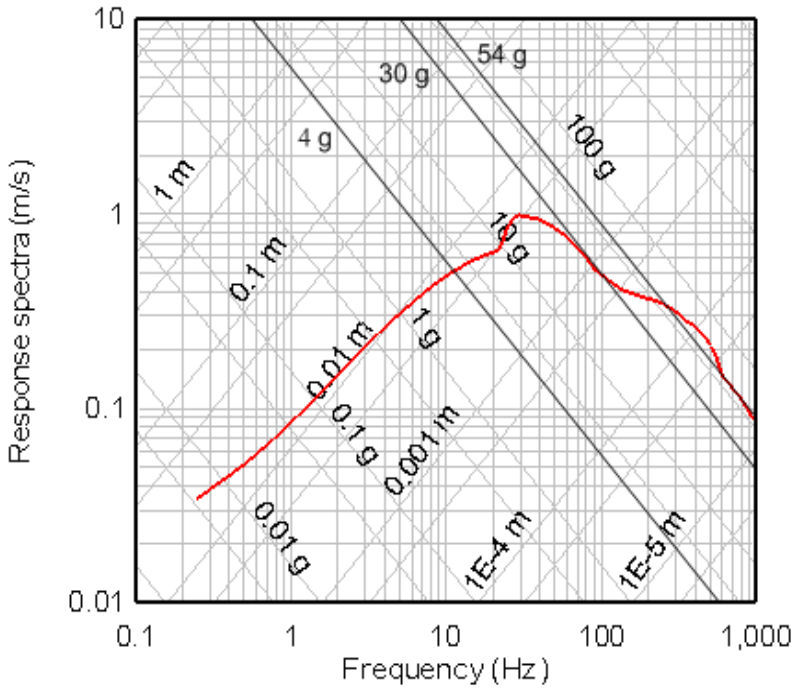

Fig. 6 Shock response spectra of equipment under in-structure shock with Kallang soil

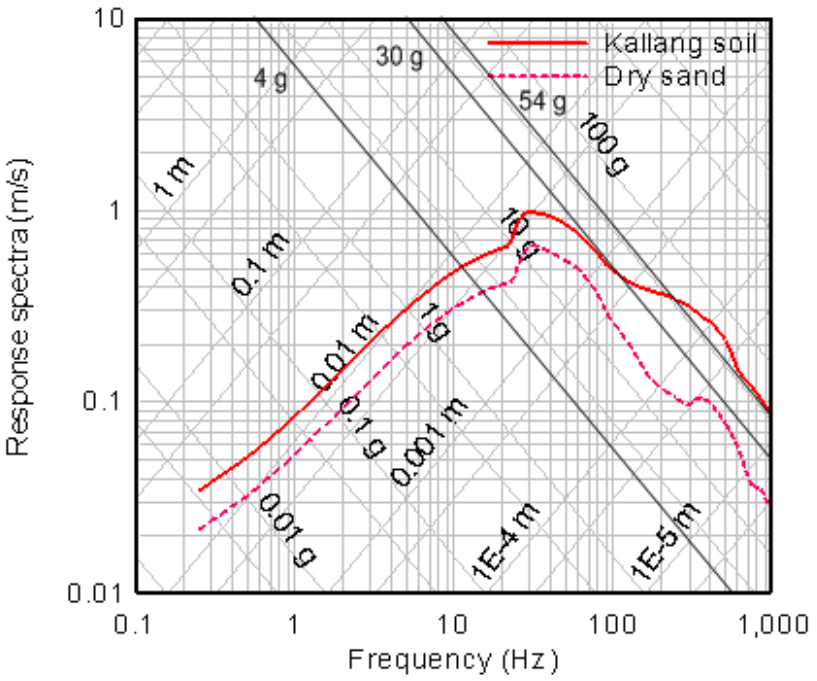

(a) Different soil

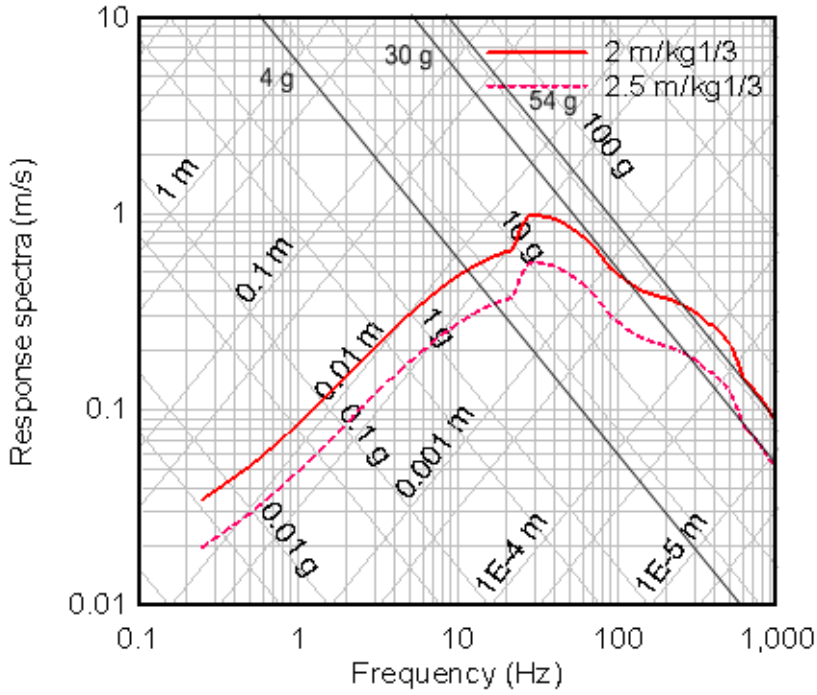

(b) Different scaled distances

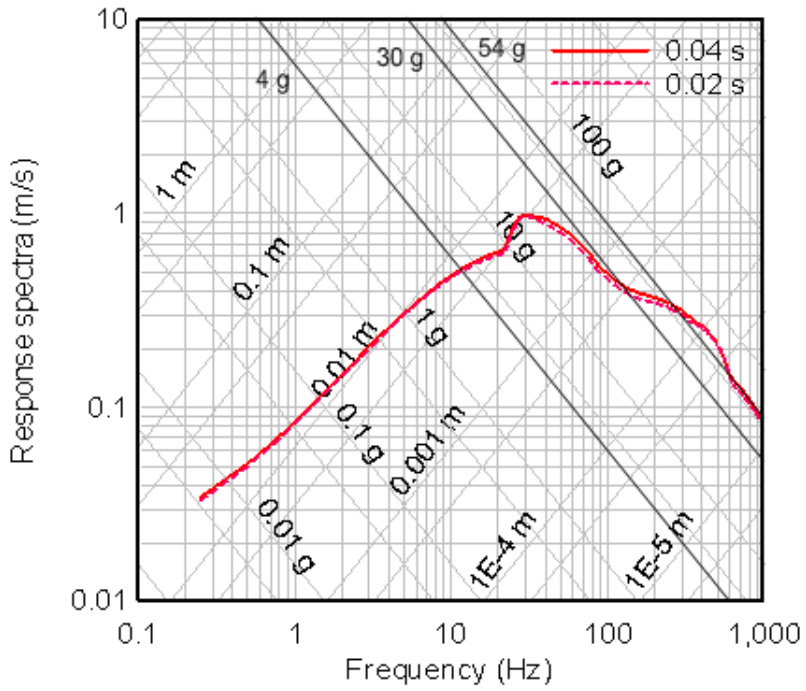

(c) Different blast time durations

Fig. 7 Influence of various factors on the shock response spectra

Table 1 Properties of typical soils in Singapore

Soil type	Density (kg/m^3)	Seismic velocity (m/s)	Attenuation coefficient
Dry sand	1633	305	2.75
Kallang soil	1420	1350	2.5
Bukit Timah soil	1800	1650	2.25

Table 2 Interfacial damping ratios of structure in typical soil

Order	In dry sand	In Kallang soil	In Bukit Timah soil
1	1.65	6.36	9.86
2	0.41	1.59	2.47
3	0.18	0.71	1.10
4	0.10	0.40	0.62
5	0.066	0.25	0.39

Table 3 Equipment shock resistance

Item	Horizontal tolerance (g's)	Vertical tolerance (g's)
Air handling units	4	4
Diesel engine generators	30	30
Gas turbine generators	31	4
Computers	53	54